The geochemical evolution of the Gulfjellet Ophiolite Complex, west Norwegian Caledonides

BRITT HESKESTAD, NINA H. HOFSHAGEN, HARALD FURNES & ROLF-BIRGER PEDERSEN

Heskestad, B., Hofshagen, N. H., Furnes, H. & Pedersen, R.-B.: The geochemical evolution of the Gulfjellet Ophiolite Complex, west Norwegian Caledonides. *Norsk Geologisk Tidsskrift*, Vol. 74, pp. 77–88. Oslo 1994. ISSN 0029-196X.

The earliest (N–S to NE–SW striking) dykes and pillow lavas of the Lower Ordovician Gulfjellet Ophiolite Complex are dominated by N-MORB to IAT-type affinities; the IAT-type seems to become more abundant with time. This development is thought to reflect spreading-related magmatism in a 'supra-subduction' zone environment. Boninitic magmatism, represented by dominantly NE–SW to E–W trending dykes, post-dates the N-MORB and IAT, and suggests formation in a fore-arc setting. The occurrence of a few MORB-type dykes cutting boninite dykes may indicate formation of new oceanic crust, possibly associated with arc splitting. The rare occurrence of post-MORB calc-alkaline magmatic activity may indicate a maturing stage of arc magmatic activity.

B. Heskestad, Amoco Norway Oil Company, P.O. Box 388, 4001 Stavanger, Norway; N. H. Hofshagen, Den norske stats oljeselskap, a.s., P.O. Box 300, 4001 Stavanger, Norway; H. Furnes & R.-B. Pedersen, Geologisk Institutt, Allegt. 41, 5007 Bergen, Norway

Introduction

Within the Upper Allochthon of the Scandinavian Caledonides, a number of ophiolite fragments are present from Karmøy to Lyngen (e.g. Dunning & Pedersen 1987; Pedersen et al. 1988; 1992; Sturt & Roberts 1991), of which the Gulfjellet Ophiolite Complex is one (Fig. 1A). The Gulfjellet Ophiolite Complex forms part of the Major Bergen Arc, a subdivision of the Bergen Arc System (Kolderup & Kolderup 1940). The Bergen Arc System comprises the Øygarden Gneiss Complex, the Minor Bergen Arc, the Ulriken Gneiss Complex, the Anorthosite Complex and the Major Bergen Arc (Fig. 1B) (Fossen 1986). The ages of the rocks of the Bergen Arc System range from Precambrian to Lower Paleozoic (Kolderup & Kolderup 1940, Sturt et al. 1975, Ryan & Skevington 1976, Dunning & Pedersen 1987).

Spreading-related magmatism within the Scandinavian Caledonides occurred in two distinct events, i.e. a Lower Ordovician phase and an Upper Ordovician to Lower Silurian phase (e.g. Dunning & Pedersen 1987; Pedersen et al. 1988, 1992). During the first phase, which lasted for some 20–30 Ma, a system of island arcs and associated marginal basins developed and can be traced along the entire length of the orogenic belt. The magmatic products of this phase show a pronounced variation from metabasalts of MORB, IAT, boninitic, calc-alkaline to alkaline composition, to granites representing the core of evolved island arc complexes (Stephens et al. 1985; Furnes et al. 1988; Pedersen & Hertogen 1990; Pedersen & Furnes 1991). The second phase represents predominantly a rifting process, occasionally with evidence of the initial stages of small oceanic basin development (Stevens et al. 1985; Furnes et al. 1990; Pedersen et al. 1991).

In this paper we present the results of a detailed geological and geochemical investigation of the Lower Ordovician Gulfjellet Ophiolite Complex in the area between Lønningdal and Svinningen (Fig. 1C).

General geology of the Major Bergen Arc

The Lower Palaeozoic sequence of the Major Bergen Arc is divided into the Gulfjellet Ophiolite Complex, the Samnanger Complex and the Os Group (Naterstad 1976, Sturt & Thon 1976; Færseth et al. 1977; Thon 1985a,b; Ingdahl 1989). The Gulfjellet Ophiolite Complex comprises a plutonic zone of layered metagabbro cumulates that gradually passes upwards into isotropic metagabbros, followed by a predominantly N–S to NE–SW trending dyke complex, with pillow lavas as the highest member. Previous geochemical work (Inderhaug 1975; Furnes et al. 1982; Thon 1985a) has shown MORB characteristics influenced by island arc magmatism. Two U/Pb age determinations of the Gulfjellet Ophiolite Complex (Dunning & Pedersen 1987) have yielded ages of 489 ± 3 Ma (plagiogranite as a MORB fractionate), and $482\ +6/-2$ Ma (tonalite). The Samnanger Complex to the east, and tectonostratigraphically underlying the Gulfjellet Ophiolite Complex, is a melange consisting of sediments hosting various components of the latter. Unconformably overlying the Gulfjellet Ophiolite Complex and the Samnanger Complex is the Os Group comprising coarse conglomerate at its base, followed by limestone, phyllite and sandstone. The limestone contains a shelly fauna of Ashgill age (Kolderup & Kolderup 1940), whereas the phyllites (of the Ulven area) contain graptolites of Early Llandovery age (Ryan & Skevington 1976; Bruton & Harper 1988).

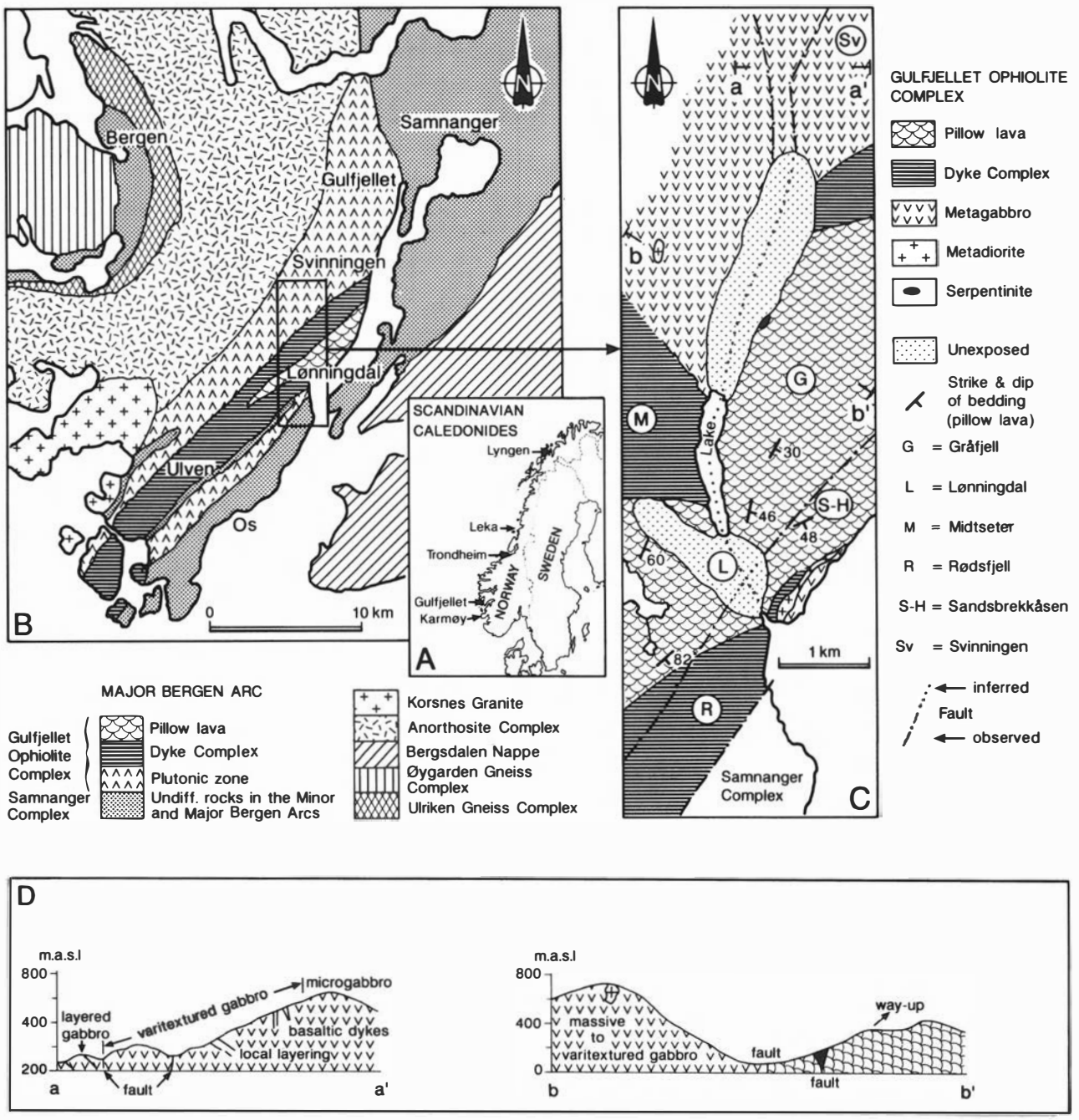

Fig. 1. Simplified geological map (B) of the Bergen Arc System (after Fossen 1986). The geological map (C) to the right shows the part of the Gulfjellet Ophiolite Complex that is the basis for this study. Map A shows some of the major ophiolite occurrences in Norway that are of similar age to the Gulfjellet Ophiolite Complex.

The Gulfjellet Ophiolite Complex

Fig. 1C shows the distribution of rock types in the investigated area. The major part of these are metagabbros, which vary from layered to massive, occurring in the northwestern part, a dyke complex in the central to southern part and pillow lavas in the eastern to southern part. Only minor occurrences of ultramafic and acid rocks are found. The distribution of rock types indicates younging to the southeast, which is corroborated by way-up in the pillow lavas.

Serpentinite

A small body of serpentinite is located within the pillow lava, bound by tectonic zones. Strong shearing and serpentinization have obliterated the original features in this body, and it is impossible to say whether it is of mantle origin or a crustal cumulate.

Metagabbro

The metagabbro sequence is best demonstrated in the northern part of the mapped area (Fig. 1C), and is shown

in the profile of Fig. 1D. Small-scale (a few cm) layered metagabbro, with moderate (30–40°) to steep, easterly dipping layering, occurs in the western part of the profile. In the layered metagabbro syn-magmatic slump and trough structures are found. Associated and intercalated with the layered metagabbro are thick (several metres) layers of massive metagabbro showing poikilitic texture. The layered/massive metagabbros are separated from varitextured metagabbro by a fault (Fig. 1C). The varitextured metagabbro shows abrupt as well as gradual textural changes from fine to coarse to pegmatitic grain sizes. Locally, within the varitextured metagabbro, diffuse, small-scale layered or laminated (on a mm scale) metagabbro occurs. Higher in the stratigraphy the varitextured metagabbro grades into a microgabbro. Within the varitextured metagabbro is the scattered occurrence of metabasalt dykes, which become more abundant upwards. Within the microgabbro, structures reminiscent of pillow lavas are found. These structures can be traced from joints in the microgabbro into well-defined 'pseudopillows'. We believe that these structures originated in the microgabbro as a result of hydrothermal activity at the top of the underlying magma chamber.

Metadiorite

Metadiorite constitutes only a minor part of the plutonic rocks of the Gulfjellet Ophiolite Complex. Only two mappable bodies, one (ca. 1.2 km × 200 m) at the transition zone between high-level gabbro and dykes, and the other (ca. 400 m × 100 m) within the metagabbro, crop out (Fig. 1C). With the exception of these intrusions, only small pockets of metadiorite occur at the highest level of the metagabbro.

Dykes

The orientation and thickness of a total of 170 metabasalt dykes have been measured, mainly from the southern part of the dyke complex, i.e. in the Rødsfjell area (Fig. 1C). Their main strikes vary from N–S to NE–SW, with dips from vertical to steep towards NW. The dyke thicknesses vary, from 0.1 m to 8 m, averaging 1.3 m. A second group of dykes strike ESE–WNW to NW–SE. Strike distribution is shown in Fig. 2. A selection of field sketches of cross-cutting relationships in the Rødsfjell–Gråfjell area is shown in Fig. 3, demonstrating that NE–SE, NE–SW to E–W striking dykes generally cross-cut the N–S trending dykes. However, a few occurrences of N–S trending dykes cutting the E–W trending dykes are observed.

Pillow lava

Pillow lavas constitute an extensive part of the mapped area, and the best examples are found in the Gråfjell area

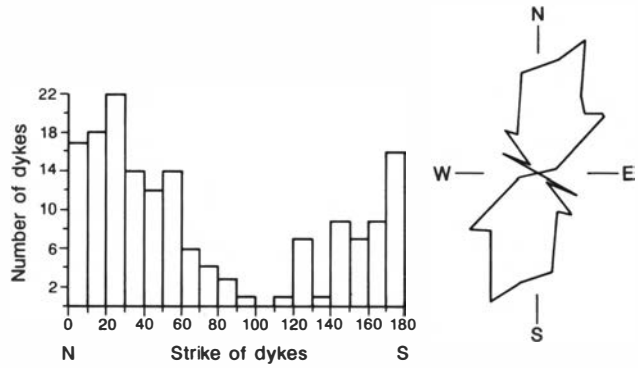

Fig. 2. Orientation of dykes shown by histogram and rose diagram.

(Fig. 1C). The size and shape of pillows varies from small (a few cm) spherical to long (>1 m) elliptical bodies. They are invariably massive and non-amygdaloidal, indicative of eruption in deep water (>1 km) (Moore 1970). Sporadic occurrences of drain-outs provide a reliable younging direction (Ballard & Moore 1977), and show that the pillow lava sequence is in a right-way-up position towards the east.

Steeply dipping metabasalt dykes, striking NNE–SSW to ENE–WSW, occur throughout the pillow lava sequence.

Petrography of the metabasalts

The metabasalt dykes and pillows are generally aphyric, but some pillows contain up to 5% plagioclase (up to 3 mm long). The pillows are fine-grained, whereas the dykes vary from fine- to medium-grained, and show ophitic texture. The dykes and pillows show greenschist facies mineral assemblages, comprising epidote, tremolite-actinolite, saussuritized plagioclase, and ore (in places surrounded by biotite).

Geochemistry

A total of 345 samples of high-level metagabbro, metabasalt dykes and pillow lavas were collected and analysed by X-ray fluorescence (XRF) at the Geological Institute, University of Bergen. The glass-bead technique of Padfield & Gray (1971) was used for the major elements and pressed powder pellets for the trace elements. International standards, with recommended values of Govindaraju (1984), were used for calibration. An additional collection of representative samples was analysed for REE, Th and Ta by ICP-MS at the Department of Earth Sciences, Memorial University of Newfoundland.

Element mobility

From a number of studies of the behaviour of elements during alteration and metamorphism of basaltic rocks, it

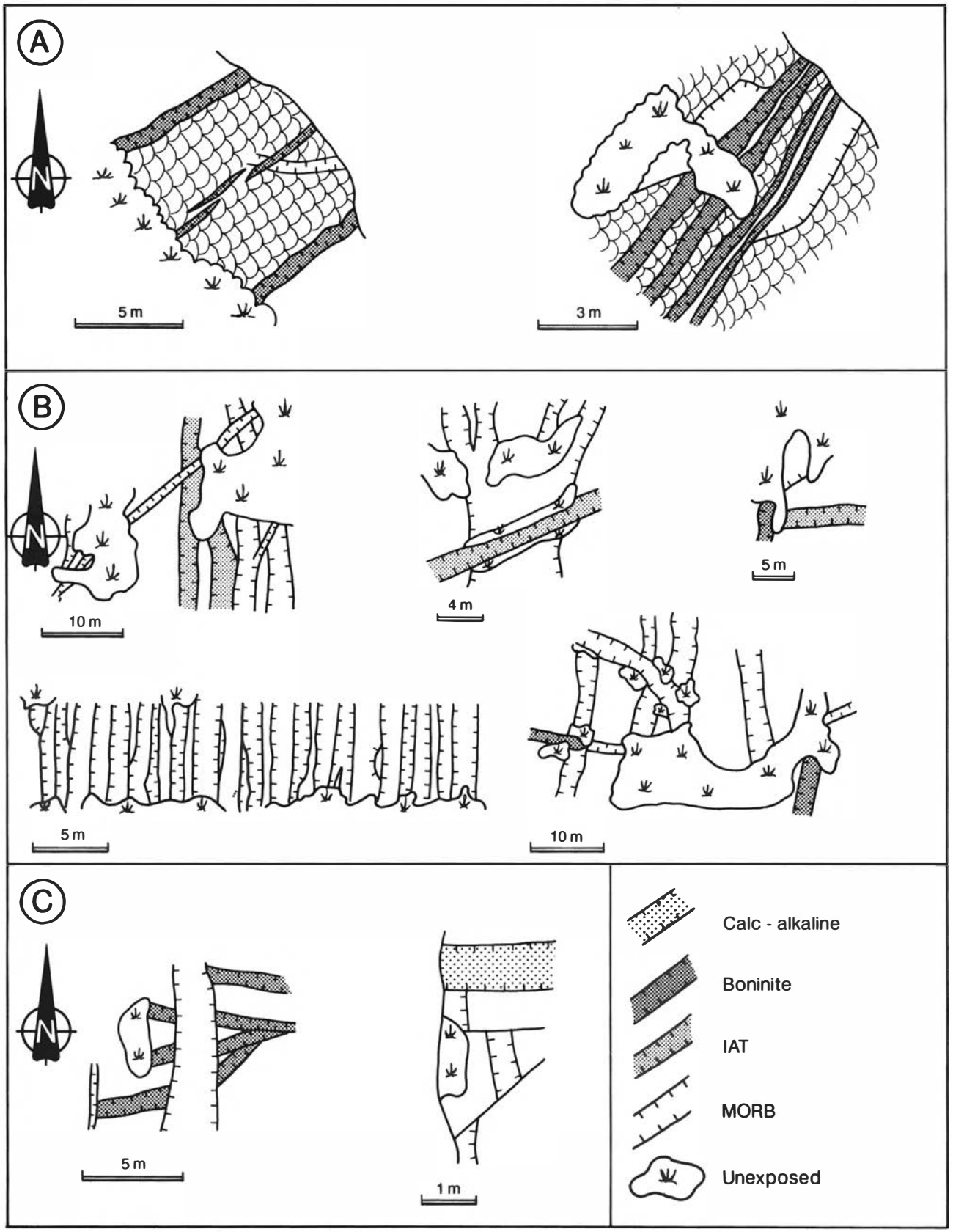

Fig. 3. Field sketches of cross-cutting dykes in the Rødsfjell–Gråfjell area: (A) in pillow lava; (B) in the dyke complex, and (C) in the high-level metagabbro.

is well demonstrated that while some elements remain relatively stable, others are lost or enriched relative to the concentration in the original rock. The mobility of an element is a function of the permeability and the extent of water–rock interaction, and the elemental solubilities in the conditions of reaction (Kelley & Delaney 1987; Bickle & Teagle 1992). The penetration of fluids into the massive metabasalt dykes was probably less compared with the pillow lavas where a substantial amount of fluid circulation might have been expected. Low temperature experimental studies of reaction between basalt and seawater have demonstrated minor leaching of Fe and enrichment of Mg (Scott & Hajash 1976; Seyfried et al. 1978). The alteration studies indicate that Al, Ti and P are the least mobilized major elements, and that Ca is variable lost. The trace elements Y, Zr, Nb, V, Cr, Co, Ni, REE, Th and Ta are generally found to be nearly immobile (e.g. Coish 1977; Hellman et al. 1979; Shervais 1982; Mottl 1983; Seyfried & Mottl 1982; Dickin & Jones 1983; Dungan et al. 1983).

The metabasaltic rocks of the Gulfjellet Ophiolite Complex

The geochemical analyses of samples of the high-level metagabbros, the metabasalt dykes and pillow lavas have shown that metabasalts of different compositions and affinities are present. This can be demonstrated by plotting in the TiO_2–Zr and Cr–Y diagrams, which discriminate mid-ocean ridge basalts (MORB) from island arc tholeiites (IAT) and within-plate basalts (WPB) (e.g. Pearce 1980) (Fig. 4). The data show significant variation in trace element contents and ratios, and concentrations typical of MORB, IAT and boninite magmas are present, with a complete gradation between the different compositions. By far the largest spread with respect to TiO_2–Zr and Cr–Y relationships is found in the dyke complex, in which magma compositions of boninitic, IAT, N-MORB to E-MORB (or WPB) affinities can be recognized. The pillow lava is dominantly N-MORB, as is the major part of the high-level metagabbro. Some metagabbros exhibit IAT-type trace element chemistries.

MORB to IAT-like. – A substantial part of the metabasalts (Table 1) from the dyke complex and all the pillow lavas can be classified as MORB, grading into IAT-like rocks (Fig. 4). The MgO content ranges from 3.35 to 10.69 wt.%. Fig. 5 shows Bowen diagrams, and with decreasing MgO, there is a marked increase in TiO_2, FeO^t, P_2O_5, Zr and Y, a marked decrease in CaO, Cr and Ni, and a slight decrease in Al_2O_3. Two samples

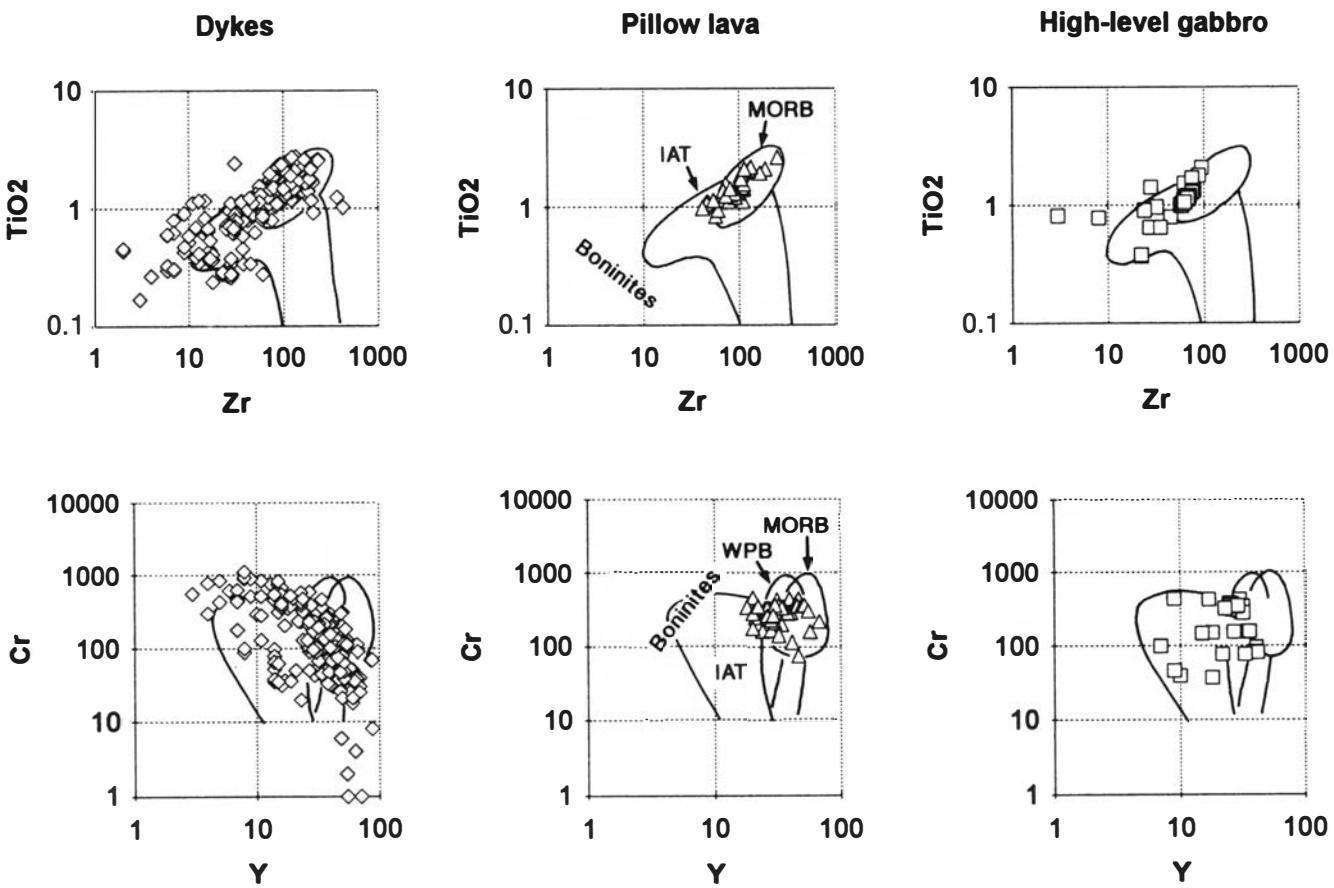

Fig. 4. All metabasalt dykes (262 samples), pillow lavas (42 samples), and a selection of high-level metagabbros (41 samples) plotted in TiO_2–Zr and Cr–Y diagrams (after Pearce 1980). The field indicated for boninites in the TiO_2–Zr diagram is based on data from Hickey & Frey (1982), Cameron et al. (1983) and Crawford et al. (1990).

Table 1. Representative major and some trace elements of MORB-type dykes and pillows from the Gulfjellet Ophiolite Complex.

Sample No.	Lithology	SiO_2	TiO_2	Al_2O_3	FeO(t)	MnO	MgO	CaO	Na_2O	K_2O	P_2O_5	LOI	Total	Cr	Ni	Y	Zr
141Q	Dyke	47.28	0.79	15.09	10.33	0.20	10.69	11.45	1.71	0.02	0.05	2.80	100.41	682	270	16	32
144I	Dyke	49.22	0.99	15.03	10.31	0.22	9.11	11.53	2.17	0.04	0.02	2.08	100.72	40	27	36	80
144L	Dyke	47.45	1.33	15.25	11.98	0.20	8.51	10.13	2.09	0.06	0.11	2.96	100.07	468	186	24	56
170C	Dyke	48.57	0.87	14.71	11.62	0.22	7.73	11.00	2.66	0.01	0.04	1.66	99.09	364	87	16	61
141B	Dyke	49.10	1.09	14.89	11.41	0.21	7.68	11.45	2.50	0.04	0.08	1.79	100.24	128	59	26	50
141E	Dyke	49.42	1.08	14.82	10.94	0.22	7.54	12.62	1.26	0.04	0.06	1.81	99.81	129	69	24	52
167A	Dyke	46.75	1.46	16.94	11.55	0.17	7.07	12.59	1.36	0.00	0.10	2.36	100.35	192	80	32	101
151G	Dyke	48.80	1.51	14.17	13.65	0.22	7.07	10.84	2.00	0.10	0.09	1.53	99.98	231	64	30	80
151F	Dyke	48.56	1.45	14.22	12.98	0.21	6.97	10.88	2.27	0.07	0.09	1.66	99.36	216	65	32	74
137F	Dyke	51.50	1.22	14.18	13.36	0.25	6.46	10.74	2.02	0.07	0.07	2.03	101.90	95	44	29	44
137H	Dyke	50.70	1.22	14.45	12.67	0.23	6.39	10.73	1.86	0.04	0.07	2.49	100.85	91	46	31	48
140I	Dyke	49.25	1.11	16.32	12.17	0.22	6.20	9.01	3.18	0.06	0.06	2.55	100.13	205	27	27	52
144K	Dyke	48.58	1.85	14.36	14.12	0.24	5.67	9.85	2.62	0.13	0.12	1.70	99.24	156	34	40	78
141P	Dyke	49.08	1.31	16.14	11.91	0.21	5.59	11.73	1.92	0.04	0.08	2.17	100.18	169	73	29	58
144J	Dyke	49.15	1.97	14.37	14.98	0.36	5.36	8.48	3.31	0.20	0.13	0.83	99.14	102	36	40	72
159V	Dyke	48.75	2.70	14.33	15.63	0.20	5.22	8.70	3.86	0.05	0.12	1.20	100.76	113	28	54	124
141K	Dyke	49.92	1.86	14.48	13.76	0.26	5.11	9.32	2.88	0.10	0.12	1.36	99.17	105	25	44	83
167C	Dyke	48.93	1.98	14.56	13.98	0.20	5.09	9.73	2.60	0.04	0.15	2.53	99.79	33	27	38	119
140D	Dyke	50.19	1.93	14.45	14.20	0.28	5.05	8.79	3.30	0.07	0.07	1.12	99.45	79	30	50	106
141A	Dyke	51.77	1.85	14.73	14.50	0.26	4.94	7.81	4.23	0.13	0.13	1.06	101.41	75	30	46	93
144H	Dyke	50.32	2.10	14.35	14.13	0.32	4.88	8.81	2.95	0.12	0.19	1.23	99.40	115	40	51	104
140F	Dyke	49.84	2.56	13.80	15.55	0.29	4.30	10.49	1.62	0.12	0.18	1.53	100.28	49	13	52	113
140H	Dyke	49.79	2.60	14.22	15.64	0.31	4.28	10.53	0.29	0.03	0.20	2.68	100.57	64	22	51	117
137B	Dyke	51.27	2.62	13.73	14.63	0.22	4.15	10.62	1.44	0.04	0.26	1.16	100.14	54	25	58	167
144C	Dyke	50.35	2.35	14.09	16.06	0.30	4.14	7.54	3.72	0.11	0.20	0.80	99.66	48	16	48	96
1371	Dyke	51.50	2.21	14.84	15.29	0.20	4.06	7.43	4.76	0.12	0.18	0.43	101.02	38	20	47	87
139A	Dyke	51.80	2.28	14.26	15.66	0.31	3.73	7.12	4.27	0.13	0.19	0.93	100.68	39	9	52	106
137A	Dyke	50.91	2.56	14.37	15.21	9,23	3.57	9.33	2.46	0.05	0.28	0.93	99.90	36	19	63	175
137C	Dyke	52.95	2.11	13.64	13.96	0.26	3.39	10.81	0.52	0.06	0.34	1.56	99.60	39	13	65	131
170B	Dyke	53.37	2.14	14.15	13.77	0.25	3.35	6.73	4.21	0.06	0.15	0.47	98.65	21	16	61	196
213	Pillow lava	47.02	0.80	16.34	9.40	0.16	9.56	13.25	1.84	0.01	0.08	1.42	99.88	456	130	20	56
191	Pillow lava	48.39	1.10	14.73	10.80	0.18	8.32	13.01	2.07	0.04	0.10	0.95	99.69	429	80	31	69
306	Pillow lava	48.11	1.25	15.23	11.09	0.18	7.31	14.11	1.94	0.05	0.14	0.89	100.30	336	87	35	81
304	Pillow lava	48.59	2.12	15.26	12.36	0.20	7.07	12.10	2.24	0.07	0.21	1.37	101.59	207	88	30	185
56	Pillow lave	47.53	1.51	14.37	12.19	0.21	6.99	14.54	1.97	0.04	0.13	0.69	100.17	276	65	38	97
273	Pillow lava	48.44	1.77	14.19	12.66	0.20	6.86	11.44	2.55	0.08	0.14	0.99	99.32	277	60	20	106
52	Pillow lava	47.60	1.31	14.90	10.64	0.20	6.84	15.10	1.89	0.04	0.13	0.76	99.41	334	75	33	86
263	Pillow lava	48.08	0.92	16.24	10.25	0.19	6.42	15.08	1.67	0.06	0.09	0.93	99.93	253	97	29	41
270	Pillow lava	47.20	2.10	14.74	14.38	0.23	5.74	12.53	1.98	0.30	0.17	0.76	100.13	258	58	26	130
277	Pillow lava	50.39	2.78	12.84	15.14	0.25	5.05	8.02	3.30	0.15	0.37	0.62	98.91	76	27	46	246

LOI: loss on ignition, FeO(t): total iron. Major oxides in wt%; trace elements in parts per million.

have considerably higher Zr contents at given MgO values than the other samples (Fig. 5), and may on this basis be classified as E-MORB.

The rare earth elements (REE) and trace elements (Th, Ta, Ce, P, Zr, Sm, Ti, Y, Yb, Sc and Cr) of representative samples of dykes (Table 4) are plotted in chondrite-normalized and MORB-normalized spider diagrams, respectively (Fig. 6). The REE diagrams of the dykes show a flat pattern from Lu to Sm, 10–20 × chondrite, and from Nd to La a progressive depletion in La, to values as low as 6 × chondrite. The REE patterns of the pillow lavas vary from nearly flat, slightly enriched in LREE (10–20 × chondrite), to patterns similar to those of the dykes described above, though with greater La depletion (1.4 × chondrite). The spider diagrams of the dykes show flat to slightly upward convex patterns between Yb and P, with Ti and Y representing the maximum normalized values. Some samples show pronounced, whereas others show only small negative Ta anomalies. The pillow lava samples show variable significant variation in trace element behavior, such as: (1) slightly progressive enrichment from Yb to Th (around 1 to 2 × MORB); (2) MORB concentrations from Yb to P, and depleted with respect to Ce, Ta and Th; and (3) low concentrations of all elements (0.3 to 0.5 × MORB), with pronounced Ta depletion.

IAT to boninitic to calc-alkaline. – Fig. 5 shows the IAT samples (Table 2) plotted in Bowen diagrams. In contrast to the typical MORB samples, the IAT samples show only a slight increase in the TiO_2, FeO^t, P_2O_5, Zr and Y contents with decreasing MgO, and their concentrations are considerably lower than those of the MORB. Al_2O_3 shows a marked increase with decreasing MgO. The other element plots (MgO vs. CaO, Cr and Ni) are similar to those of MORB composition. Fig. 7 shows the REE and trace element spider diagrams for IAT-type metabasalts. Element concentrations are shown in Table 4. In the REE diagram all the samples show a progressive depletion from Lu to La, the latter showing the largest range (4.3–1.3 × chondrite). In the spider diagram there is a progressive depletion from Yb to Ta, and

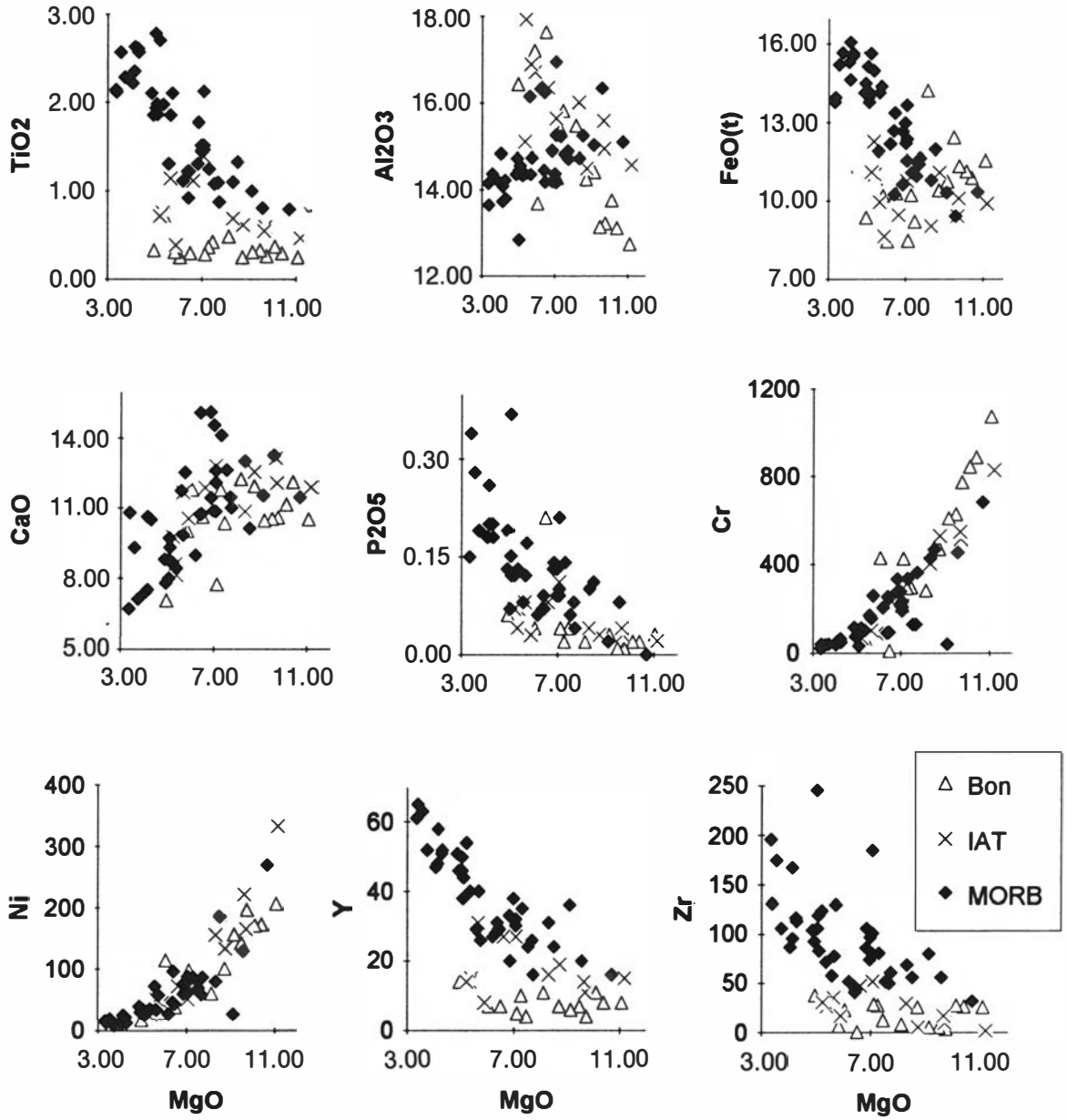

Fig. 5. Bowen diagram showing relationship between MgO vs. TiO_2, Al_2O_3, FeO^t, CaO, CaO/Al_2O_3, P_2O_5, Cr, Ni Zr and Y, for MORB, IAT and metaboninite dykes and pillow lavas of the Gulfjellet Ophiolite Complex.

Table 2. Representative major and some trace elements of IAT-type dykes from the Gulfjellet Ophiolite Complex.

Sample No.	Lithology	SiO_2	TiO_2	Al_2O_3	FeO(t)	MnO	MgO	CaO	Na_2O	K_2O	P_2O_5	LOI	Total	Cr	Ni	Y	Zr
144N	Dyke	47.61	0.46	14.58	9.88	0.18	11.18	11.89	1.63	0.02	0.02	2.49	99.94	827	334	15	2
141C	Dyke	48.01	0.59	14.94	10.08	0.23	9.70	12.08	1.94	0.03	0.03	1.69	99.32	515	166	11	10
140E	Dyke	48.43	0.54	15.58	9.41	0.16	9.65	13.13	1.27	0.01	0.04	2.43	100.65	546	222	14	17
139B	Dyke	50.10	0.61	14.49	11.08	0.22	8.74	12.54	0.57	0.02	0.03	2.28	100.68	527	134	19	6
145J	Dyke	49.49	0.68	16.01	9.02	0.22	8.31	10.84	2.45	0.09	0.04	2.16	99.31	405	156	16	30
263A	Dyke	49.33	1.39	15.64	10.76	0.16	7.07	12.81	1.92	0.05	0.11	1.02	100.26	212	51	27	52
72B	Dyke	49.90	1.11	16.35	9.45	0.14	6.62	11.87	2.98	0.06	0.08	1.36	99.92	232	73	27	48
259A	Dyke	52.48	0.38	16.71	8.64	0.14	5.90	10.55	3.47	0.07	0.03	0.79	99.16	88	45	8	17
75B	Dyke	49.68	1.14	16.88	9.96	0.12	5.66	11.65	2.98	0.02	0.08	0.83	99.00	101	51	31	36
137E	Dyke	51.48	0.72	17.92	11.03	0.18	5.40	8.13	2.00	0.01	0.07	3.36	100.30	63	26	15	27
200A	Dyke	51.71	0.75	15.11	12.28	0.18	5.35	8.63	4.28	0.03	0.04	1.49	99.85	79	35	14	31
137D	Dyke	50.62	0.71	18.35	11.11	0.18	5.23	9.79	2.17	0.01	0.07	3.06	101.30	66	28	14	31

LOI: loss on ignition, FeO(t): total iron. Major oxides in wt%; trace elements in parts per million.

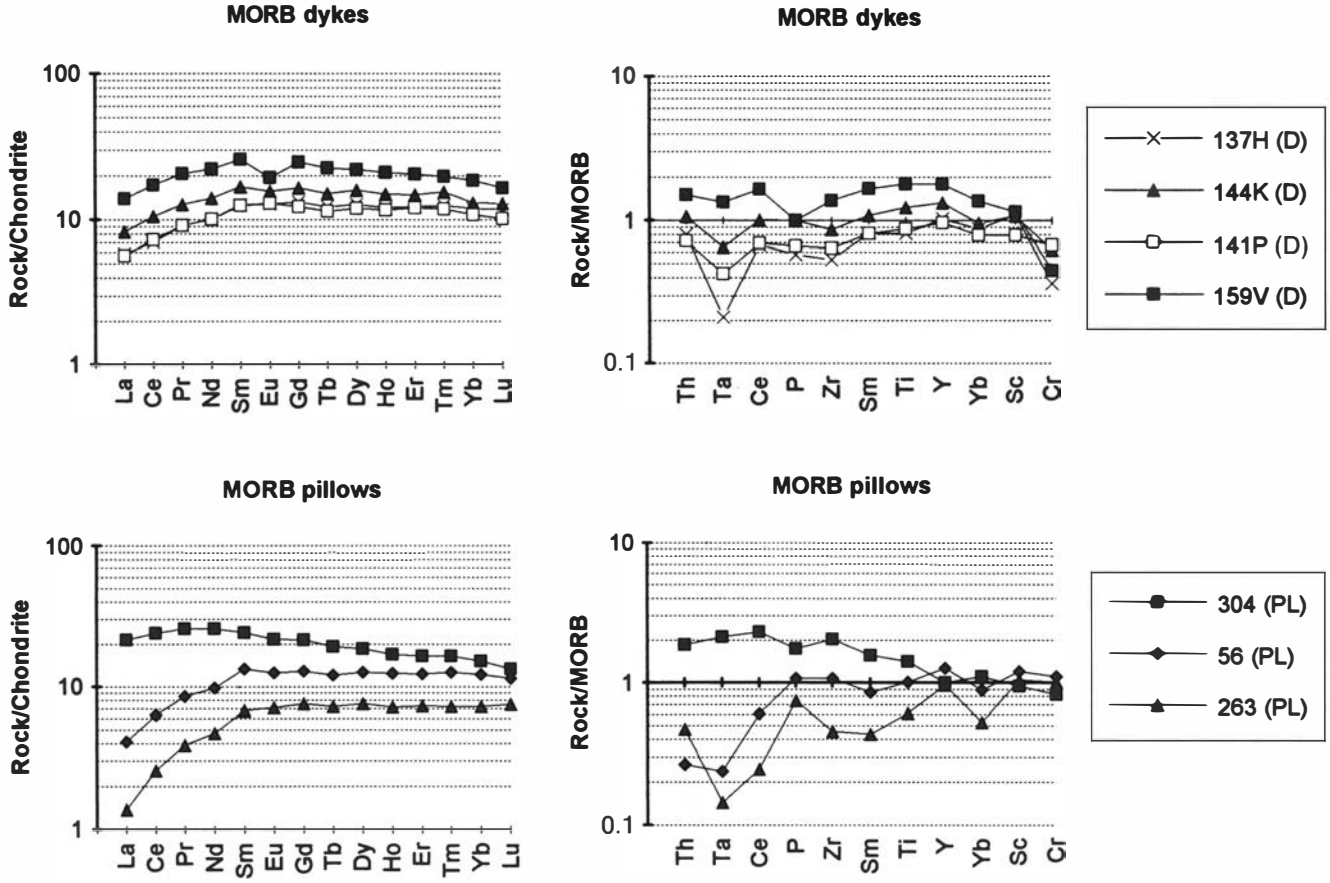

Fig. 6. Chondrite-normalized REE- and MORB-normalized spider diagrams of representative MORB samples (metabasalt dykes and pillow lava) of the Gulfjellet Ophiolite Complex. Chondrite values (in ppm): La = 0.330, Ce = 0.88, Pr = 0.112, Nd = 0.60, Sm = 0.181, Eu = 0.069, Gd = 0.249, Tb = 0.047, Dy = 0.31, Ho = 0.070, Er = 0.200, Tm = 0.030, Yb = 0.200, Lu = 0.034 (after Haskin et al. 1968). MORB values (in ppm when not wt% shown): Th = 0.20 (Tarney et al. 1981), Ta = 0.18, Ce = 10, P_2O_5 = 0.12 wt%, Zr = 90, Sm = 3.3, TiO_2 = 1.50 wt%, Y = 30, Yb = 3.4, Sc = 40, Cr = 250 (after Pearce 1980).

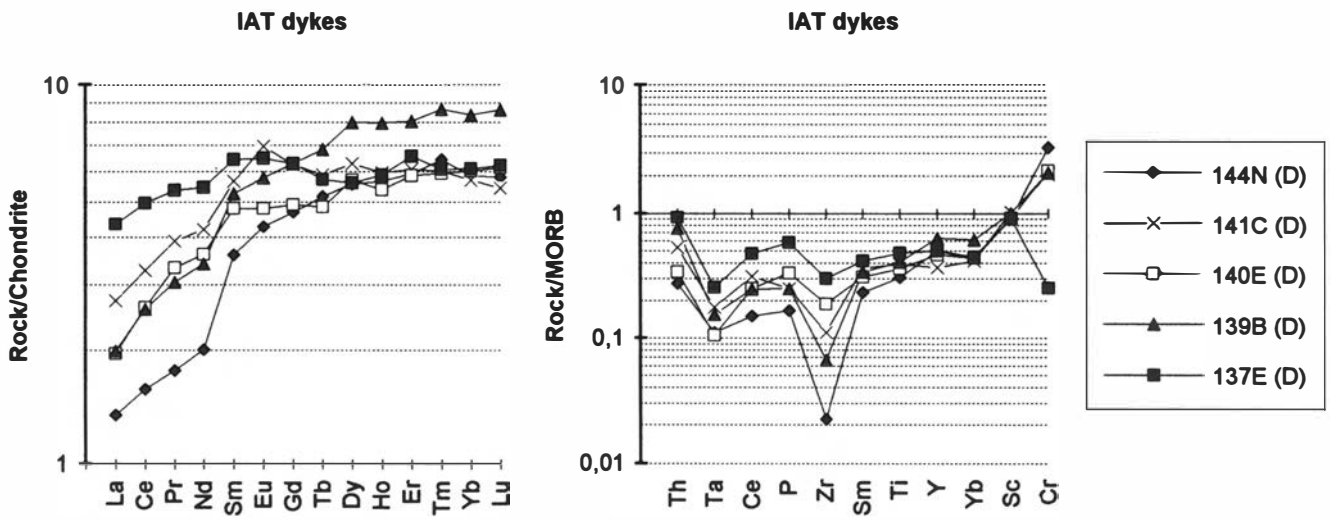

Fig. 7. Chondrite-normalized REE- and MORB-normalized spider diagrams of representative IAT-type samples of the Gulfjellet Ophiolite Complex. Normalized values as in Fig. 6.

with significant negative Zr anomalies for all samples. Th is moderately enriched, resulting in a negative Ta anomaly. All element concentrations are markedly lower than the MORB-type metabasalts shown in Fig. 6.

Boninitic samples (Table 3) are plotted on Bowen diagrams in Fig. 5. They show similar trends to those defined by the IAT samples with respect to MgO vs. Al_2O_3, CaO, P_2O_5, Zr and Y, but generally the concentrations are lower, in particular with respect to Y. TiO_2 is very low and stays flat with decreasing MgO, whereas there is a marked decrease in FeO^t. Other elements (Cr and Ni) show, similar to the IAT samples, approximately

Table 3. Representative major and some trace elements of boninite-type and calc-alkaline dykes from the Gulfjellet Ophiolite Complex.

Sample No.	Lithology	SiO_2	TiO_2	Al_2O_3	FeO(t)	MnO	MgO	CaO	Na_2O	K_2O	P_2O_5	LOI	Total	Cr	Ni	Y	Zr
56F	Bon. dyke	49.34	0.25	12.74	11.55	0.19	11.07	10.51	2.19	0.04	0.03	1.33	99.24	1074	208	8	26
56G	Bon. dyke	49.87	0.29	13.12	10.88	0.19	10.39	12.11	1.60	0.01	0.02	1.10	99.58	888	174	8	27
56A	Bon. dyke	49.74	0.37	13.76	11.13	0.19	10.10	11.15	2.06	0.02	0.02	1.23	99.77	844	172	11	28
87D	Bon. dyke	50.58	0.26	13.22	11.34	0.19	9.74	10.60	2.60	0.02	0.01	1.35	99.91	773	198	4	4
87C	Bon. dyke	50.28	0.33	13.14	12.43	0.19	9.48	10.56	2.43	0.12	0.01	0.92	99.89	628	144	7	6
87B	Bon. dyke	51.12	0.31	14.41	10.74	0.18	9.15	10.47	2.60	0.08	0.03	1.06	100.15	609	157	6	6
52A	Bon. dyke	50.96	0.25	14.24	10.40	0.18	8.72	11.93	2.32	0.04	0.03	0.72	99.79	473	101	7	26
140G	Bon. dyke	47.14	0.48	15.48	14.22	0.24	8.13	12.24	1.38	0.17	0.02	2.00	101.50	283	61	11	9
141N	Bon. dyke	52.64	0.42	15.82	9.21	0.17	7.46	10.36	2.08	0.02	0.04	2.46	100.68	297	73	4	13
53A	Bon. dyke	50.99	0.36	15.39	10.22	0.18	7.27	11.78	2.43	0.06	0.02	0.75	99.45	294	70	10	28
144B	Bon. dyke	56.02	0.28	14.27	8.48	0.14	7.12	7.75	2.89	0.02	0.04	2.21	99.22	427	98	5	29
144EF	Bon. dyke	50.84	0.29	17.63	10.28	0.18	6.51	10.62	1.83	0.02	0.21	3.06	101.47	11	39	7	1
140B	Bon. dyke	54.03	0.25	13.69	8.46	0.17	6.06	11.80	2.68	0.03	0.04	1.13	98.34	432	115	7	23
144F	Bon. dyke	51.08	0.31	17.19	10.21	0.18	5.85	10.03	1.23	0.01	0.03	3.20	99.32	99	29	8	7
191A	Bon. dyke	52.66	0.33	16.43	9.35	0.18	4.96	7.08	4.23	0.03	0.06	2.49	97.80	97	17	14	38
249B	Calc. dyke	50.89	0.93	15.34	9.60	0.15	4.72	10.67	2.81	0.86	0.68	1.14	97.79	51	18	27	208

LOI: loss on ignition, FeO(t): total iron. Major oxides in wt%; trace elements in parts per million.

Table 4. Trace element analyses of representative samples of MORB, IAT and boninites from the Gulfjellet Ophiolite Complex.

Sample No.	Affinity	La	Ce	Pr	Nd	Sm	Eu	Gd	Tb	Dy	Ho	Er	Tm	Yb	Lu	Th	Ta	Sc
137H (D)	MORB	2.192	6.765	1.246	7.187	2.687	1.115	4.056	0.711	4.834	1.024	3.057	0.445	2.959	0.448	0.159	0.038	43.7
144K (D)	MORB	3.109	10.118	1.749	9.969	3.58	1.364	5.04	0.88	6.072	1.271	3.708	0.554	3.252	0.492	0.214	0.118	43
141P (D)	MORB	2.127	6.995	1.256	7.172	2.676	1.132	3.754	0.666	4.567	0.99	3.003	0.421	2.696	0.387	0.145	0.077	31.7
159V (D)	MORB	5.239	16.481	2.831	15.804	5.519	1.693	7.594	1.31	3.172	1.787	5.103	0.705	4.628	0.628	0.302	0.241	45.8
304 (PL)	MORB	8.076	22.942	3.529	18.306	5.17	1.89	6.599	1.119	7.054	1.435	4.099	0.587	3.77	0.509	0.374	0.381	37.9
56 (PL)	MORB	1.538	6.072	1.174	6.968	2.839	1.094	3.947	0.701	4.827	1.061	3.074	0.45	3.02	0.434	0.053	0.043	48
263 (PL)	MORB	0.515	2.465	0.532	3.334	1.44	0.617	2.328	0.422	2.893	0.611	1.816	0.259	1.796	0.287	0.095	0.026	42.1
144N (D)	IAT	0.506	1.51	0.242	1.429	0.766	0.372	1.431	0.299	2.119	0.481	1.473	0.229	1.451	0.221	0.055	0.02	36.6
141C (D)	IAT	1.02	3.125	0.536	2.985	1.205	0.606	1.908	0.341	2.396	0.506	1.514	0.214	1.413	0.207	0.106	0.032	41.1
140E (D)	IAT	0.738	2.495	0.456	2.568	1.021	0.417	1.504	0.281	2.17	0.457	1.457	0.211	1.492	0.234	0.068	0.019	36.7
139B (D)	IAT	0.75	2.47	0.417	2.421	1.117	0.503	1.925	0.397	3.055	0.68	2.009	0.308	2.081	0.329	0.152	0.028	40.5
137E (D)	IAT	1.633	4.743	0.734	3.876	1.368	0.564	1.926	0.332	2.131	0.5	1.637	0.216	1.511	0.237	0.185	0.046	36.1
140G (D)	BON	0.847	2.264	0.36	1.782	0.702	0.362	1.077	0.21	1.589	0.398	1.472	0.293	2.499	0.455	0.114	0.201	43.4
141N (D)	BON	0.639	1.788	0.274	1.577	0.564	0.281	0.786	0.137	0.891	0.202	0.576	0.092	0.607	0.098	0.071	0.046	35.7
144B (B)	BON	2.314	5.82	0.823	4.068	1.215	0.435	1.521	0.271	1.889	0.429	1.276	0.206	1.424	0.229	0.482	0.071	50.3
144EF (D)	BON	0.89	2.138	0.287	1.401	0.472	0.206	0.799	0.135	1.054	0.241	0.728	0.119	0.815	0.141	0.2	0.02	42.5
140B (D)	BON	0.847	2.264	0.36	1.782	0.702	0.362	1.077	0.21	1.589	0.398	1.472	0.293	2.499	0.455	0.114	0.201	43.4
144F (D)	BON	0.702	1.625	0.224	1.101	0.332	0.163	0.517	0.102	0.781	0.171	0.613	0.086	0.655	0.099	0.177	0.017	25.9

Trace elements in parts per million. D: dyke; PL: pillow lava.

the same trends as defined by the MORB samples. Following Crawford et al. (1990) and Arculus et al. (1992), the boninitic dykes of the Gulfjellet Ophiolite Complex are classified as predominantly high-Ca boninites, grading into intermediate-Ca boninites.

The metaboninites of the Gulfjellet Ophiolite Complex show a variety of REE patterns (Fig. 8), from a nearly flat, slightly convex downward pattern (6 × chondrite), to a slight to strong progressive depletion from Lu to La, with the highest variation in Lu (12–26 × chondrite). This is the opposite pattern of depletion to that observed for the IAT samples. Three samples show slight positive Eu anomalies. In the spider diagrams, a downward convex pattern is displayed between Sc and Th, with the minima in Sm and Zr. Both positive and negative Ta anomalies are shown. Such an element distribution is characteristic of boninites (e.g. Murton et al. 1992).

One sample (249B in Table 3) shows a typical calc-alkaline geochemical signature with a much higher Zr content (208 ppm) at a relatively low TiO_2 (0.93 wt.%).

Magmatic affinity versus dyke orientation. – Around 80% of the MORB dykes strike N–S to NE–SW, with a clear dominance of the former. IAT dykes generally have the same orientation as the MORB-type dykes, whereas the metaboninites dominantly strike NE–SW to E–W. In general, dykes with MORB and IAT compositions are cut by metaboninite dykes. Examples of a N–S-striking MORB dyke cutting a metaboninite dyke and an E-W-oriented calc-alkaline dyke cutting a MORB dyke have been found. However, since MORBs both pre- and post-date metaboninites, the relationship between the metaboninites and the calc-alkaline dyke can only be inferred.

Relationship between pillow lava and dykes. – The pillow lava sequence is cut by dykes of MORB, IAT and

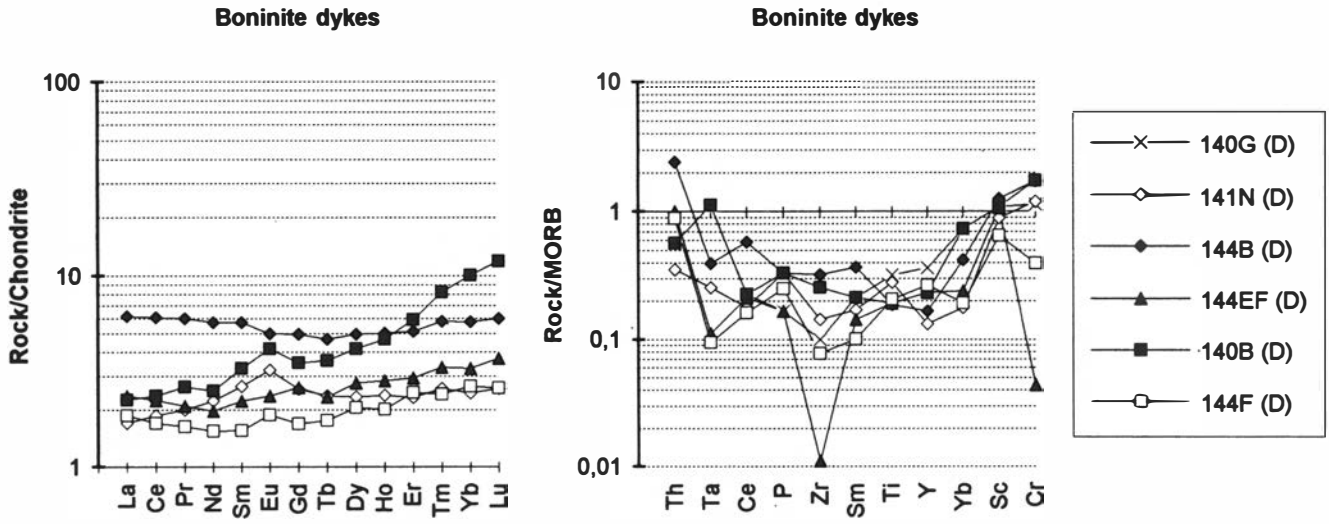

Fig. 8. Chondrite-normalized REE- and MORB-normalized spider diagrams of representative metaboninite samples of the Gulfjellet Ophiolite Complex. Normalized values as in Fig. 6.

boninitic compositions, of which the MORB and boninitic are the dominant. The pillows are dominantly of MORB compositions, grading into typical IAT types. No boninitic pillows have been found. This would indicate that the boninitic-type magmatism post-dates the MORB and IAT types.

Comparison of the magmatic evolution between the Gulfjellet Ophiolite Complex and other time-equivalent ophiolites in Norway

From Karmøy to Lyngen a number of Lower Ordovician, arc-related ophiolite fragments (Fig. 1) developed during the time period 470–500 Ma (Dunning 1987; Dunning & Pedersen 1987). The magmatic development of the Gulfjellet Ophiolite Complex, as far as we can trace it, is very similar to two of these complexes, i.e. the Karmøy and Leka ophiolites. The well-constrained magmatic evolution of the Karmøy Ophiolite Complex (Pedersen & Hertogen 1990) shows the following development: formation of (1) MORB/IAT, (2) bonninites, (3) IAT, (4) calc-alkaline to, finally, alkaline magmas (Pedersen & Hertogen 1990). An approximately similar magmatic development, though not so well constrained owing to limited age control, can be demonstrated for the Leka Ophiolite Complex (Furnes et al. 1988, 1992). As documented above, on the basis of the cross-cutting relationships in the dyke complex and of the dyke/pillow lava relations, the first stage in the magmatic evolution of the Gulfjellet Ophiolite Complex was production of MORB and IAT, followed by boninitic magmatism. Timing constraints of this magmatic evolution are unavailable for the Gulfjellet Ophiolite Complex, but for the Karmøy Ophiolite Complex the timespan from typical MORB to boninitic magmatism is of the order of 10–15 Ma (Dunning & Pedersen 1987). The general evolution of the Karmøy Ophiolite Complex, in which the calc-alkaline magmatism represents a very late stage of the magmatic evolution, may justify the suggestion that the calc-alkaline dyke in the Gulfjellet Ophiolite Complex represents the latest phase of magmatism.

Discussion and conclusions

The magmatic products of the Gulfjellet Ophiolite Complex show, at all evolutionary stages, an inherited island arc influence. In a series of papers, geotectonic models based on the relationship between geochemistry, ages and regional setting of the Caledonide ophiolites (e.g. Pedersen et al. 1988, 1992; Pedersen & Furnes 1991) indicate that the earliest ophiolitic axis sequences formed at spreading centres in convergent plate margin tectonic setting. The magmatism at this stage, in which N-MORB to IAT-type rocks were formed, may be considered as having occurred in a 'supra-subduction zone' setting, producing SSZ ophiolites in the terminology of Pearce et al. (1984). The most appropriate example of relatively young to present-day island arc and associated back-arc basin evolution, where the above-mentioned magmatic types are represented, is the West Philippine–Mariana region (Crawford et al. 1981).

The N–S to NNE–SW trending dykes of predominantly MORB character, but also with abundant IAT-type compositions, are thought to have formed in a 'supra-subduction zone' environment (Fig. 9). It is interesting to note that the proportion of typical MORB to typical IAT varies considerably within the Lower Ordovician ophiolites in Norway. Whereas in the Karmøy and Gulfjellet ophiolite complexes there is a high proportion of IAT-type magmatic products, further north, in the Trondheim area, there is considerably less evidence of this type (Furnes et al. 1985). An explanation may be found in the modern Lau Basin, where the spreading axis is oblique to the subduction zone (Collier & Sinha 1990).

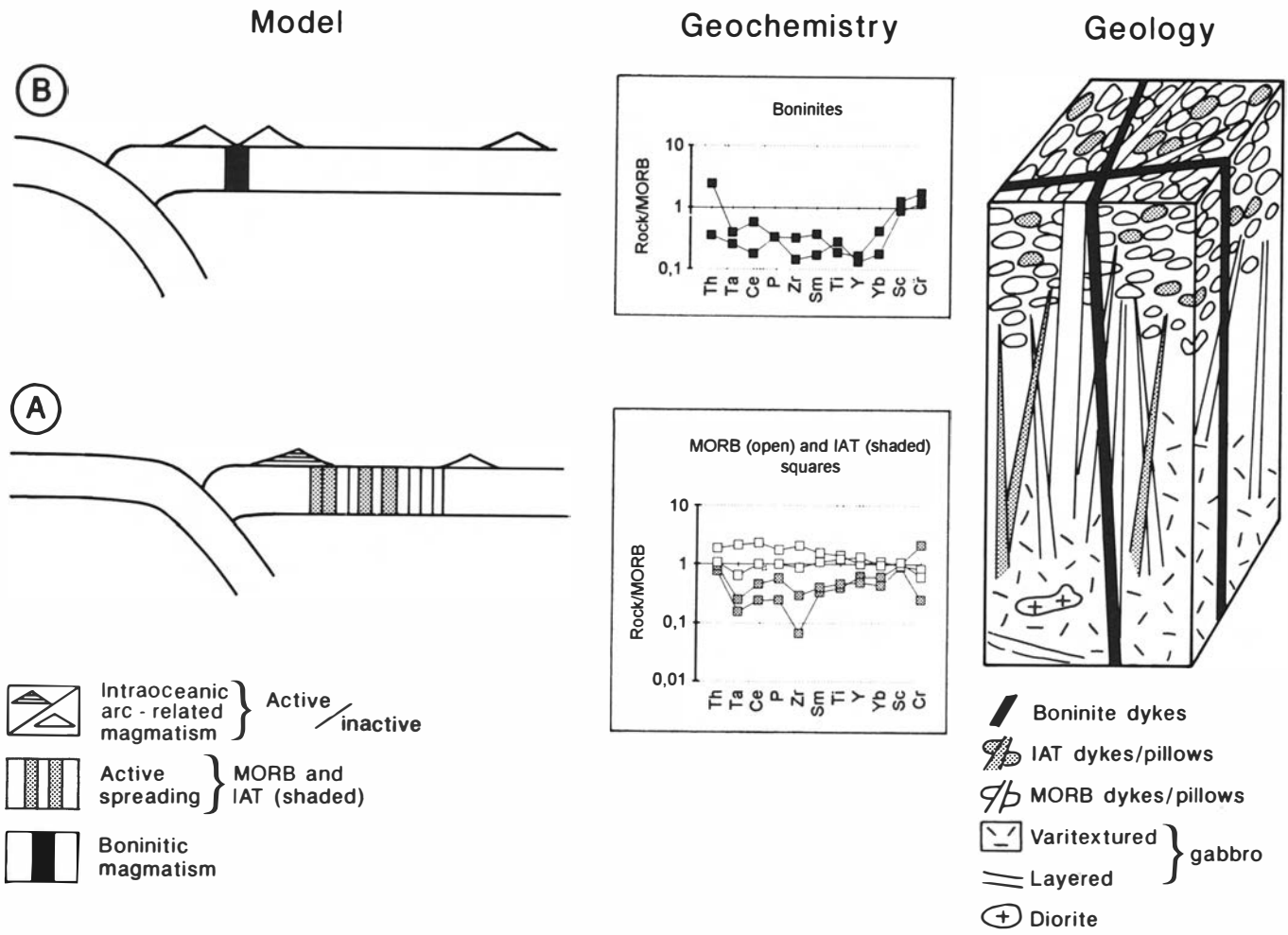

Fig. 9. Summary of geological and geochemical features of the Gulfjellet Ophiolite Complex, on the basis of which a model is proposed. (A) The earliest recorded stage of the Gulfjellet Ophiolite Complex, represented by metabasalt dykes and pillow lavas of MORB and IAT compositions, takes place by spreading above a subduction zone. The tendency of the abundance of IAT to increase with time may be the result of progressive depletion of the source by repeated melting. (B) Later development of boninitic magmatism, represented by dykes cutting the MORB and IAT metabasalt dykes and pillows of the earlier stage. The general lowering in the concentration levels of Yb, Y, Ti, Sm and Zr shows a further depletion of the source area. However, at this stage there is also a relative enrichment in Th and Ta, showing that the source is getting enriched in the most imcompatible elements during subduction.

In such a setting, time-equivalent spreading-axis basalts would show different trace element patterns ranging from typical MORB to IAT depending on the distance from the subduction zone. The ophiolite complexes in which the first magmatic products show a high IAT/MORB ratio, like the Gulfjellet and Karmøy ophiolite complexes, would thus have to be formed at a spreading axis close to the subduction zone.

Subsequent intrusion of boninitic magmas in the Karmøy Ophiolite Complex, documented to have taken place some 10–15 Ma after the MORB/IAT magmatism (Pedersen & Hertogen 1990), would indicate that this magmatism took place in a fore-arc region, since modern examples of these chemistries have been found only in that setting (i.e. Reagan & Meijer 1983). It is further suggested that this magmatic event may have formed in conjunction with arc splitting and formation of new back-arc crust, by comparison with young ensimatic arc systems (Crawford et al. 1981). This development, well documented for the Karmøy Ophiolite Complex, also represents a substantial part of the magmatic development of the Gulfjellet Ophiolite Complex, and a similar general geotectonic model should therefore be applicable (Fig. 9). The further general late-stage development of calc-alkaline and alkaline magmatism, indicative of a maturing arc setting and evolved back-arc basin demonstrated in the Karmøy and Leka ophiolite complexes, is not well documented for the Gulfjellet Ophiolite Complex, though there is some sparse evidence of late-stage calc-alkaline magmatism.

Acknowledgements. – Financial support for this study has been provided through grants from the University of Bergen and the Norwegian Research Council for Science and the Humanities. We thank D. A. H. Teagle for comments on an early draft of this paper, and the reviewers J. Malpas and S. Bergman and an anonymous reviewer. J. Ellingsen helped with the preparation of illustrations.

Manuscript received October 1993

References

Arculus, R. R., Pearce, L. A., Murton, B. J. & van der Laan, S. R. 1992: Igneous stratigraphy and major-element geochemistry of Holes 786A and 786B. *In* Fryer, P., Pearce, J. A., Stokking, L. B. et al.: *Proceeding of the Ocean Drilling Program, Scientific Results, vol. 125*, 143–169.

Ballard, R. D. & Moore, J. G. 1977: *Photographic Atlas of the Mid-Atlantic Rift Valley*. Springer-Verlag, New York, 144 pp.

Bickle, M. J. & Teagle, D. A. H. 1992: Strontium alteration in the Troodos ophiolite: implications for fluid fluxes and geochemical transport in mid-ocean ridge hydrothermal systems. *Earth and Planetary Science Letters 113*, 219–237.

Bruton, D. L. and Harper, D. A. T. 1988: Arenig–Llandovery stratigraphy and faunas across the Scandinavian Caledonides. *In* Harris, A. L. & Fettes, D. J. (eds.): *The Caledonian-Appalachian Orogen*. Geological Society, Special Publication No. 38, pp. 247–268.

Cameron, W. B., McCulloch, M. T. & Walker, D. A. 1983: Boninite petrogenesis: chemical and Nd-Sr isotropic constraints. *Earth and Planetary Science Letters 65*, 75–89.

Coish, R. A. 1977: Ocean floor metamorphism in Betts Cove Ophiolite, Newfoundland. *Contributions to Mineralogy and Petrology 60*, 255–270.

Collier, J. & Sinha, M. 1990: Seismic images of a magma chamber beneath the Lau Basin back-arc spreading centre. *Nature 346*, 646–648.

Crawford, A. J., Beccaluva, L. & Serri, G. 1981: Tectono-magmatic evolution of the West Philippine-Mariana region and the origin of boninites. *Earth and Planetary Science Letters 54*, 346–356.

Crawford, A. J., Fallon, T. J. & Green, D. H. 1990: Classification, petrogenesis and tectonic setting of boninites. *In* Crawford, A. J. (ed.): *Boninites*. Unwin Hyman, 352 pp.

Dickin, A. P. & Jones, N. W. 1983: Relative element mobility during hydrothermal alteration of a basic sill, Isle of Skye, NW Scotland. *Contributions to Mineralogy and Petrology 82*, 147–153.

Dungan, M. A., Vance, J. A. & Blanchard, D. P. 1983: Geochemistry of the Shuksan greenschists and blueschists, North Cascades, Washington: variably fractionated metabasalts of oceanic affinity. *Contributions to Mineralogy and Petrology 82*, 131–146.

Dunning, G. R. 1987: U/Pb zircon ages of Caledonian ophiolites and arc sequences: Implications for tectonic setting. *Terra Cognita 7*, 179.

Dunning, G. R. & Pedersen, R. B. 1987: U/Pb zircon ages of Caledonian ophiolites and arc-related plutons of the Norwegian Caldeonides: Implications for development of Iapetus. *Contributions to Mineralogy and Petrology 98*, 13–23.

Færseth, R. B., Thon, A., Larsen, S. G., Sivertsen, A. & Elvestad, L. 1977: Geology of the Lower Palaeozoic rocks in the Samnanger-Osterøy area, Major Bergen Arc, western Norway. *Norges Geologiske Undersøkelse 334*, 19–58.

Fossen, H. 1986: Structural and metamorphic development of the Bergen area, Western Norway. Unpublished Cand. Scient. thesis, University of Bergen.

Furnes, H., Pedersen, R.-B. & Stillman, C. J. 1988: The Leka Ophiolite Complex, Central Norwegian Caledonides: field characteristics and geotectonic significance. *Journal of the Geological Society, London 145*, 145–412.

Furnes, H., Pedersen, R. B., Hertogen, J. & Albrektsen, B. A. 1992: Magma development of the Leka Ophiolite Complex, central Norwegian Caledonides. *Lithos 27*, 259–277.

Furnes, H., Thon, A., Nordås, J. & Garmann, L. B. 1982: Geochemistry of Caledonian metabasalts from some Norwegian ophiolite fragments. *Contributions to Mineralogy and Petrology 79*, 295–307.

Furnes, H., Ryan, P. D., Grenne, T., Roberts, D., Sturt, B. A. & Prestvik, T. 1985: Geological and geochemical classification of the ophiolite fragments in the Scandinavian Caledonides. *In* Gee, D. G. & Sturt, B. A. (eds.): *The Caledonide Orogen – Scandinavia and Related Areas*, pp. 657–670.

Furnes, H., Skjerlie, K. P., Pedersen, R. B., Andersen, T. B., Stillman, C. J., Suthren, R., Tysseland, M. & Garmann, L. B. 1990: The Solund-Stavfjord Ophiolite Complex and associated rocks, west Norwegian Caledonides: Geology, geochemistry and tectonic environment. *Geological Magazine 127*, 209–229.

Govinadaraju, K. 1984: 1984 compilation of working values and sample description for 170 international reference samples of mainly silicate rocks and minerals. *Geostandards Newsletters, vol. VIII*, Special Issue, July.

Haskin, L. A., Haskin, M. A., Frey, F. A. & Wildeman, T. R. 1968: Relative and absolute terrestrial abundances of the rare earths. *In* Ahrens, L. H. (ed.): *Origin and Distribution of the Elements*, pp. 889–912, Pergamon, New York.

Hellman, P. L., Smith, R. E. & Hendersson, P. 1979: The mobility of the rare earth elements: evidence and implications from selected terrains affected by burial metamorphism. *Contributions to Mineralogy and Petrology 71*, 23–44.

Hickey, R. L. & Frey, F. A. 1982: Geochemical characteristics of boninite series volcanics: Implications for their source. *Geochimica et Cosmochimica Acta 46*, 2099–2115.

Inderhaug, J. E. 1975: Liafjell områdets geologi. Unpublished Canad. real. thesis, University of Bergen.

Ingdahl, S. E. 1989: The Upper Ordovician – Lower Silurian rocks in the Os area, Major Bergen Arc, Western Norway. *Norsk Geologisk Tidsskrift 69*, 163–175.

Kelley, D. S. & Delaney, J. R. 1987: Two-phase separation and fracturing in mid-ocean ridge gabbros at temperatures greater than 700°C. *Earth and Planetary Science Letters 83*, 53–56.

Kolderup, C. F. & Kolderup, N. H. 1940: Geology of the Bergen Arcs. *Bergen Museum Skrifter nr. 20*, 137 pp.

Moore, J. G. 1970: Water content of basalt erupted on the ocean floor. *Contributions to Mineralogy and Petrology 28*, 272–279.

Mottl, M. D. 1983: Metabasalt, axial hot springs, and structure of hydrothermal systems at mid-oceanic ridges. *Geological Society of America, Bulletin 94*, 161–180.

Murton, B. J., Peate, D. W., Arculus, R. J., Pearce, J. A. & van der Laan, S. 1992: Trace element geochemistry of volcanic rocks from Site 786: the Izu-Bonin forearc. *In* Fryer, P., Pearce, J. A., Stokking, L. B. et al.: Proceeding of the Ocean Drilling Program, Scientific Results, *vol. 125*, 211–235.

Nasterstad, J. 1976: Comment on the Lower Paleozoic unconformity. West Norway. *American Journal of Science 276*, 394–397.

Padfield, T. & Gray, A. 1971: Major element rock analyses by X-ray fluorescence – a simple fusion method. N. V. Philips, Eindhoven, Analytical Equipment, FS35.

Pearce, J. A. 1980: Geochemical evidence for the genesis and eruptive setting of lavas from Tethyan ophiolites. *In* Panayiotou, A. (ed.): *Ophiolites*. Geological Survey Department, Cyprus, 261–272.

Pearce, J. A., Lippard, S. J. & Roberts, S. 1984. Characteristics and tectonic significance of supra subduction-zone ophiolites. *In* Kokelaar, B. P. & Howells, M. F. (eds.). *Marginal Basin Geology. Volcanic and associated sedimentary and tectonic processes in modern and ancient marginal basins*. Geological Society of London, Special Publication no. 16, Blackwell, Oxford, 77–94.

Pedersen, R. B. & Furnes, H. 1991: Geology, magmatic affinity and geotectonic environment of some Caledonian ophiolites. *Journal of Geodynamics 13* nos. 2–4, 183–203.

Pedersen, R. B. & Hertogen, J. 1990: Magmatic evolution of the Karmøy Ophiolite Complex, SW Norway; Relationship between MORB–IAT–boninitic–calc-alkaline and alkaline magmatism. *Contributions to Mineralogy and Petrology 104*, 271–293.

Pedersen, R. B., Bruton, D. L. & Furnes, H. 1992: Ordovician faunas, island arcs and ophiolites in the Scandinavian Caledonides. *Terra Nova 4*, 217–222.

Pedersen, R. B., Furnes, H. & Dunning, G. R. 1988: Some Norwegian ophiolite complexes reconsidered. *Norges Geologiske Undersøkelse, Special Publications no. 3*, 80–85.

Pedersen, R. B., Furnes, H. & Dunning, G. R. 1991: The age of the Sulitjelma Gabbro, north Norway: Further evidence for the development of a Caledonian marginal basin in Ashgillian/Llandoverian time. *Geological Magazine 128*, 141–153.

Reagan, M. & Meijer, A. 1983: Geology and geochemistry of early arc volcanic rocks from Guam. *Geological Society of America, Bulletin 95*, 701–713.

Ryan, P. D. & Skevington, D. 1976: A reinterpretation of the Late Ordovician – Early Silurian stratigraphy of the Dyvikvågen and Ulven–Vaktdal areas, Hordaland, western Norway. *Norges Geologiske Undersøkelse 324*, 1–19.

Scott, R. B. & Hajash, A. Jr. 1976: Initial submarine alteration of basaltic pillow lavas: A microprobe study. *American Journal of Science 276*, 480–501.

Seyfried, W. E., Mottl, M. & Bischoff, J. L. 1978: Seawater/basalt effects on the chemistry and mineralogy of spilites from the ocean floor. *Nature 275*, 211–213.

Seyfried, W. E. & Mottl, M. J. 1982: Hydrothermal alteration of basalt by seawater under seawater-dominated conditions. *Geochimica et Cosmochimica Acta 46*, 985–1002.

Shervais, J. W. 1982: Ti-V plots and the petrogenesis of modern and ophiolitic lavas. *Earth and Planetary Science Letters 59*, 101–118.

Stephens, M. B., Furnes, H., Robins, B. & Sturt, B. A. 1985: Igneous activity within the Scandinavian Caledonides. *In* Gee, D. G. & Sturt, B. A. (eds.): *The Caledonide Orogen – Scandinavia and Related Areas*, pp. 623–656. John Wiley & Sons.

Sturt, B. A. & Roberts, D. 1991: Tectonostratigraphic relationships and obduction histories of Scandinavian ophiolite terranes. *In* Peters, Tj. et al. (eds.): *Ophiolite Genesis and Evolution of the Oceanic Lithosphere*, pp. 745–69. Ministry of Petroleum and Minerals, Sultanate of Oman.

Sturt, B. A. & Thon, A. 1976: The age of orogenic deformation in the Swedish Caledonides, a discussion. *American Journal of Science 276*, 385–390.

Sturt, B. A., Skarpenes, O., Ohanian, A. T. & Pringle, I. R. 1975: Reconnaissance Rb/Sr isochron study in the Bergen Arc System and regional implications. *Nature 253*, 595–599.

Tarney, J., Saunders, A. D., Mattey, D. P., Wood, D. A. & Marsh, B. D. 1981: Geochemical aspects of back-arc spreading in the Scotia Sea and Western Pacific. *Philosophical Transactions of the Royal Society, London A 300*, 263–285.

Thon, A. 1985a. The Gullfjellet ophiolite complex and the structurel evolution of the major Bergen arc, west Norwegian Caledonides. *In* Gee, D. G. & Sturt, B. A. (eds.). *The Caledonide Orogen – Scandinavia and Related Areas*, pp. 671–677.

Thon, A. 1985b. Late Ordovician and Early Silurian cover sequences to the west Norwegian ophiolite fragments: stratigraphy and structural evolution. *In* Gee, D. G. & Sturt, B. A. (eds.): *The Caledonide Orogen – Scandinavia and Related Areas*, pp. 407–415. John Wiley & Sons.